# THE ASSEMBLY OF A PHOTOLUMINESCENT NANOCOMPLEX BASED ON UPCONVERSION NANOPARTICLES

*S. Shanwar*[1], *L. Liang*[2], *A.V. Nechaev*[3], *I.V. Balalaeva*[1], *V.A. Vodeneev*[1], *A.V. Zvyagin*[1, 2, 4], *E.L. Guryev*[1]

[1] Institute of Biology and Biomedicine, Lobachevsky State University of Nizhny Novgorod, Nizhny Novgorod, 603950, Russia;
[2] ARC Centre of Excellence «Nanoscale BioPhotonics», Department of Physics and Astronomy, Macquarie University, Sydney 2109, Australia;
[3] Department of Chemistry and Technology of Biologically Active Compounds, Medical and Organic Chemistry, M.V. Lomonosov Institute of Fine Chemical Technologies, MIREA - Russian Technological University, 119571 Moscow, Russia;
[4] The Institute of Molecular Medicine, I.M. Sechenov First Moscow State Medical University, 119991 Moscow, Russia.

**Abstract.** Over the past two decades, developments in the field of nanobiomedicine have come a long way despite the unresolved hindrances. The creation and development of effective theranostic agents based on nanomaterials are urgent needs of modern medicine. Upconversion nanoparticles (UCNP) appear to be the most promising agents for developing theranostics due to their unique optical properties. There has been extensive research on new approaches to obtain stable colloids capable of prolonged circulation in the bloodstream, particularly with bovine serum albumin (BSA). The present work contributes to solving the problem of obtaining stable agents based on UCNP by coating water-soluble UCNP-NOBF4 with a stable protein corona layer of BSA. The assembled nanocomplex is promising for usage as a diagnostic agent and is set for further investigation.

**Keywords:** Upconversion nanoparticle, Protein corona, Bovine serum albumin.

**List of Abbreviations**

UCNP – Upconversion nanoparticles
UCNP-OA – Oleic Acid capped UCNP
UCNP-NOBF4 – Nitrosonium tetrafluoroborate coated UCNP
NIR – Near Infrared
PL – Photoluminescence
EPR effect – Enhanced permeability and retention effect
PC – Protein Corona
BSA – Bovine serum albumin
μM – Micromolar
nm – nanometer
DMF – Dimethylformamide
TEM – Transmission electron microscope
DLS – Dynamic light scattering
ELS – Electrophoretic light scattering
PDI – Polydispersity Index

## Introduction

Nowadays, the application of nanoparticles in biomedicine is an actively and rapidly developing research area. They are considered promising candidates, especially for optical imaging (Deyev & Lebedenko, 2017). Their successful biomedical application is bound by specific requirements, including biocompatibility, biodegradability, colloidal stability, and prolonged blood circulation (Aires et al., 2015).

Upconversion nanoparticles (UCNP) particularly have emerged amongst other nanoparticles for their unique and superior optical properties. The homogenous core and shell crystal structure of UCNP significantly increases the upconversion rate and upconversion coefficient in aqueous solutions (Wang et al., 2010; Zhou et al., 2012). Moreover, the trivalent lanthanide ion dopants ($Yb^{3+}$, $Tm^{3+}$, $Er^{3+}$) of the core grant these UCNP the capability of excitation in the near-infrared (NIR) range and emission in the NIR, visible or ultraviolet regions (Li et al., 2015). Their exceptional features, alongside the prolonged photoluminescence (PL) lifetime (up to 1 ms), facilitate the avoidance of autofluorescence interference and deep tissue penetration up to several centimeters (Chatterjee et al., 2008; Song et al., 2012; Zheng et al., 2016).

The methodology of their synthesis has been improving to achieve well-formed and monodisperse nanoparticles with high PL intensity.

However, the outcome is lipophilic nanoparticles such as oleic acid (OA) coated nanoparticles and, hence not biocompatible. Further modifications of their surfaces are necessary to obtain hydrophilic nanoparticles, for example, using the ligand exchange procedure (Chen et al., 2017). One of the most successful modifications is with the inorganic compound nitrosonium tetrafluoroborate ($NOBF_4$) with a molecular weight of 116.81 g/mol by the ligand exchange method resulting in hydrophilic nanoparticles and a relatively unaltered size as the compound is positively charged and very small (Dong et al., 2011).

Generally, nanoparticles take advantage of the passive delivery route, facilitated by the enhanced permeability and retention (EPR) effect. The EPR effect is observed in solid tumors where nanoscale materials tend to passively diffuse through the large pores of abnormal tumor vasculature and accumulate in tumor tissues more than normal tissues (Matsumura et al., 1987; Barua & Mitragotri, 2014).

Upon entering biological media, nanoparticles are quickly covered with a dynamic layer of proteins called protein corona (PC) (Cedervall et al., 2007; Lundqvist, 2013). The protein corona affects nanoparticles' physicochemical properties, such as size and charge, and determines their interaction with biological objects (Nel et al., 2009; Dominguez-Medina et al., 2016). Protein adsorption onto the nanoparticle's surface is mediated by ionic and van der Waals forces, hydrogen bonds, and hydrophobic interactions depending on the nanoparticles' characteristics (Hadjidemetriou & Kostarelos, 2017). In the last decade, there have been several studies investigating the possibility of manipulating PC to stabilize nanoparticles, and the most intensively considered protein is bovine serum albumin (BSA) due to its abundance in blood, biocompatibility, biodegradability, and long circulation time (Bern et al., 2015; An & Zhang, 2017). In this work, we have assembled a diagnostic nanocomplex based on UCNP modified with $NOBF_4$ and coated with BSA capable of up-converting NIR light into higher energy NIR and visible light.

## Materials and Methods

*Synthesis of UCNP-OA and UCNP-$NOBF_4$.*

Hydrophobic UCNP-OA core/shell structure ($NaY_{0.794}F_4$: $Yb_{0.2}Tm_{0.06}/NaYF_4$) were synthesized in Federal Research Center «Crystallography and Photonics» RAS, Russia, by solvatothermal decomposition method as described in (Mai et al., 2007, Guryev et al., 2020). The ligand exchange reaction was carried out to remove OA with $NOBF_4$ (Sigma-Aldrich, USA). A suspension of UCNP-OA in hexane (Cryochrom, Russia) (5 mg/ml) was mixed with $NOBF_4$ solution in dimethylformamide (DMF) (Sigma-Aldrich, USA) (0.01 M) at a ratio of 1:1 (v:v) and kept stirring on a magnetic stirrer overnight at room temperature. The obtained UCNP-$NOBF_4$ were pelleted by centrifugation (10000 × g, 7 min) and re-dispersed in DMF and flocculated with toluene (Himreaktiv, Russia) and hexane mixture (1:1, v:v). After flocculation, the resulting UCNP-$NOBF_4$ were collected by centrifugation (10000 × g, 7 min) and washed twice with ethanol and once with deionized water. Finally, they were dispersed in deionized water and stored at 4°C.

*Characterization of UCNP-OA and UCNP-$NOBF_4$*

The TEM image of UCNP-OA was obtained using a transmission electron microscope LEO-912 ABOMEGA (Carl Zeiss, Germany) for size and shape confirmation. The hydrodynamic diameters of UCNP-OA and UCNP-$NOBF_4$ were determined by dynamic light scattering (DLS), and the ζ-potential of UCNP-$NOBF_4$ was measured by electrophoretic light scattering (ELS), using a Zetasizer Nano ZS system (Malvern Instruments Ltd., UK) according to the manufacturer's recommendations. The PL properties of the UCNP-OA and UCNP-$NOBF_4$ were investigated using an SM 2203 spectrofluorimeter (SOLAR, Belarus) and an ATC-C4000-200AMF-980-5-F200 external semiconductor laser module with a wavelength of 980 nm (Semiconductor devices, Russia). The PL emission spectra were recorded from 400 to 850 nm wavelengths in a quartz cuvette with an optical path length of 1 cm.

*Optimization of BSA concentration for PC formation on UCNP-NOBF$_4$*

The BSA stock was prepared in deionized water by vigorous stirring and then filtered through a membrane filter (0.22 μm) to remove protein clusters. A dilution series of BSA was prepared and incubated with UCNP-NOBF$_4$ (1:1, v:v), where UCNP-NOBF$_4$ was added dropwise to the BSA suspension and mixed. The final concentrations were 0.25 mg/ml of UCNP-NOBF$_4$ and 25, 50, 75, 100 and 120 μM of BSA. The mixtures were incubated for 4 h at room temperature. The size and ζ-potential were recorded 15 min and 4 h after incubation.

## Results

*Synthesis and characterization of UCNP-OA and UCNP-NOBF$_4$*

UCNP-OA core/shell structure $NaY_{0.794}F_4$: $Yb_{0.2}$, $Tm_{0.06}$/$NaYF_4$ were synthesized with strictly controlled size and shape using the solvatothermal decomposition method and subsequently converted into UCNP-NOBF$_4$ by ligand exchange (Fig. 1) (Mai et al., 2007; Dong et al., 2011). Coordinate stabilization of lanthanide and fluorine precursors in an OA solution, after being heated in an oxygen-free environment, yields nanosized cubic UCNP crystals (α-phase crystals). The obtained hexagon-shaped and more stable UCNP (β-phase crystals) were formulated after additional heat treatment (Guryev et al., 2020). The transition of UCNP to the hexagonal phase and the subsequent formation of an inert shell from NaYF$_4$ can significantly increase their PL brightness, which is useful for in vitro and especially in vivo imaging (Generalova et al., 2017). UCNP-OA investigation by TEM confirms obtaining hexagon-shaped nanoparticles with an average size of 36 ± 2.75 nm (Fig. 2A). The hydrodynamic diameter of UCNP-OA was 67.94 ± 0.38 nm because of formation of a hydration shell around the particles, with an average polydispersity since the PDI was 0.254 ± 0.011 (Fig. 2B) (Bhattacharjee, 2016).

The hydrophobic nature of the aforementioned UCNP-OA renders them unsuitable for biological applications. Hydrophilicity was achieved via the ligand exchange method where

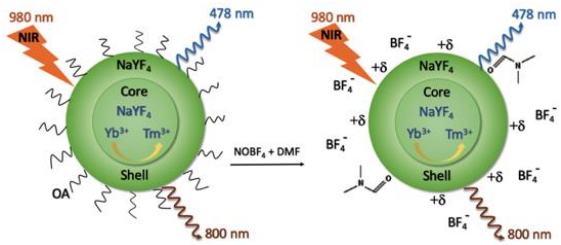


**Fig. 1.** A scheme illustrating UCNP-OA core/shell structure and the ligand exchange process converting UCNP-OA into UCNP-NOBF$_4$

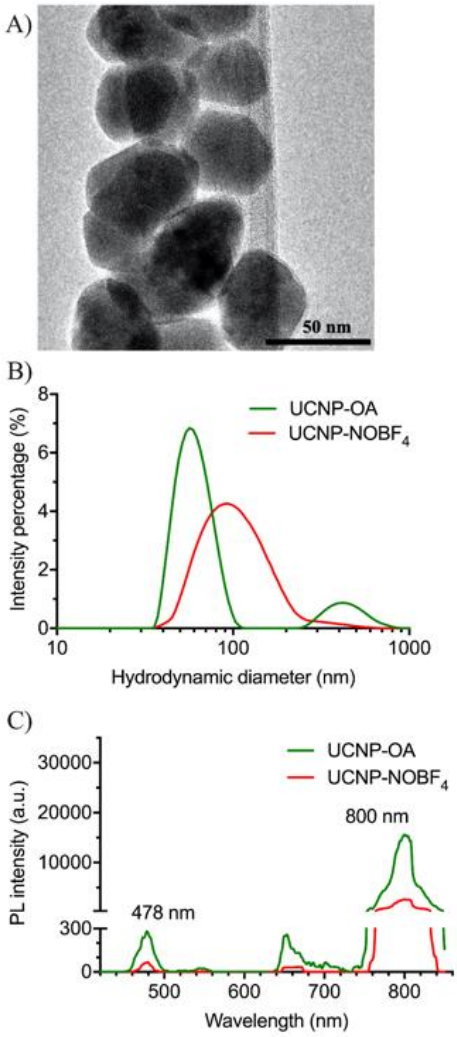


**Fig. 2.** Characterization of UCNP-OA and UCNP-NOBF$_4$ nanoparticles: A – TEM image of UCNP-OA core/shell structure ($NaY_{0.794}F_4$: $Yb_{0.2}$, $Tm_{0.06}$/$NaYF_4$), B – Hydrodynamic diameter distributions of UCNP-OA and UCNP-NOBF$_4$ obtained by DLS in hexane and deionized water, respectively, C – PL emission spectrum of UCNP-OA and UCNP-NOBF$_4$ under excitation at 980 nm

the OA residues were replaced with the small inorganic and ionic compound $NOBF_4$. Surface modification of UCNP-OA with $NOBF_4$ yielded hydrophilic nanoparticles with a hydrodynamic diameter of 93.91 ± 1.03 nm and a moderate polydispersity since PDI was 0.171 ± ± 0.020 (Fig. 2B). Both PDI value were below 0.3 showing a high level of uniformity in size and a low level of aggregation. The particles of UCNP-$NOBF_4$ were surrounded by $NO^+$ ions on the surface of UCNP and $BF_4^-$ as counterions (Fig. 1) (Dong et al., 2011). They had a positive ζ-potential of +57.2 ± 2.04 mV (Fig. 3B) that indicates high colloidal stability in suspension because the electrostatic repulsion between these positively charged nanoparticles overweighs the gravitational attraction force between particles, hence lower aggregate formation (Bhattacharjee, 2016). The PL emission peaks of both nanoparticles are in the blue (478 nm) and NIR (800 nm) regions (Fig. 2C). The latter falls within the transparency window of biological tissue (700–1100 nm), rendering them ideal for bioimaging (Li et al., 2015). Although the PL intensity of UCNP was significantly reduced after $NOBF_4$ coating, the exhibited intensity is still sufficient for bioimaging (Chen et al., 2017).

*Optimization of BSA concentration for PC formation on UCNP-$NOBF_4$*

Protein corona of BSA is used to stabilize the obtained UCNP-$NOBF_4$ prior to further investigation. The aim was to formulate a stable layer of BSA around UCNP-$NOBF_4$ shielding the particles from each other and additional proteins in biological fluids as well as increasing their blood circulation time. PC formation is a protein concentration dependent phenomenon, therefore a dilution series of BSA concentrations was assessed to determine the finest concentration for this purpose (Zhang et al., 2017). Low concentrations of BSA caused relatively high aggregation of UCNP-$NOBF_4$, whereas high concentrations led to the preservation of excess unbound protein molecules (Fig. 3A). The ζ-potential increases in absolute value with increasing albumin concentration (Fig. 3C) and higher values of ζ-potential tip the force scale in favor of electrostatic repulsion resulting in even more stable colloids. Colloidal stability, size, and ζ-potential of all suspensions were

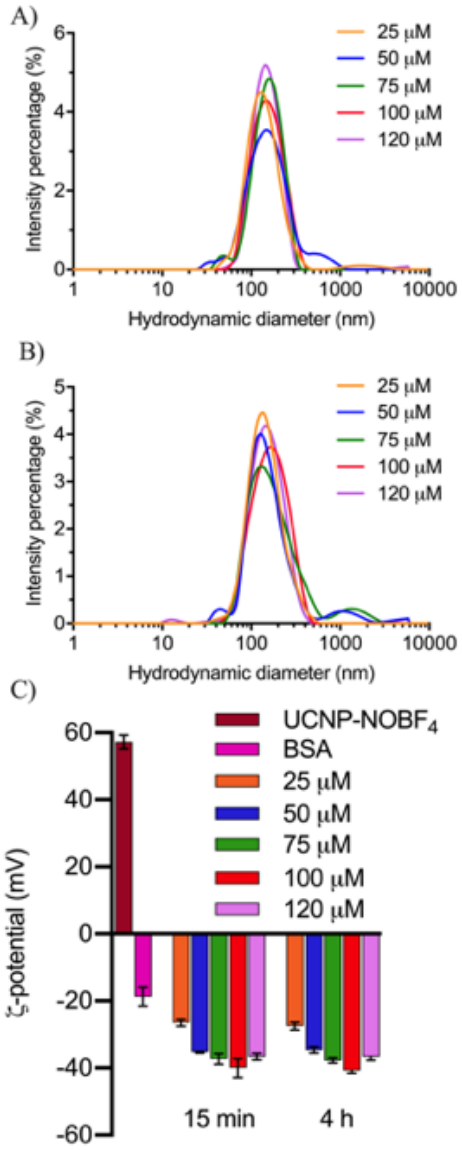


**Fig. 3.** Determination of the optimal concentration of BSA for the formation of PC on the surface of UCNP-$NOBF_4$: A, B – Hydrodynamic diameter of BSA-UCNP-$NOBF_4$ after the incubation of UCNP-$NOBF_4$ (0.25 mg/ml) with BSA at different concentrations (25–120 μM) for 15 min and 4 h at room temperature acquired by DLS, respectively. C – The ζ-potential of UCNP-$NOBF_4$, BSA, and BSA-UCNP-$NOBF_4$ recorded by ELS. All measurements were carried out in deionized water

*Table 1*

**The hydrodynamic diameter of UCNP-$NOBF_4$ incubated with different concentrations of BSA (25 – 120 μM) for 15 min and 4 h**

| Sample / Incubation time | | Hydrodynamic diameter (nm) | | PdI | |
|---|---|---|---|---|---|
| | | 15 min | 4 hours | 15 min | 4 hours |
| UCNP-$NOBF_4$ (0.25 mg/ml) Incubated with | BSA 25 μM | 116.5 ± 1.361 | 118.5 ± 1.986 | 0.271 ± 0.009 | 0.279 ± 0.012 |
| | BSA 50 μM | 120.6 ± 0.9849 | 119.4 ± 2.312 | 0.42 ± 0.006 | 0.435 ± 0.012 |
| | BSA 75 μM | 121.7 ± 5.551 | 131.6 ± 8.9 | 0.342 ± 0.046 | 0.413 ± 0.026 |
| | BSA 100 μM | 119.9 ± 0.7572 | 123.9 ± 1.553 | 0.322 ± 0.004 | 0.369 ± 0.055 |
| | BSA 120 μM | 108.7 ± 2.946 | 108.9 ± 2.042 | 0.423 ± 0.071 | 0.488 ± 0.006 |

evaluated and sustained after 4 hours of incubation (Fig. 3B, C). The best BSA concentration capable of forming a single layer of BSA around UCNP-$NOBF_4$ with minimum excess unbound albumin was 100 μM with a hydrodynamic diameter of 119.9 ± 0.9 nm, moderate polydispersity, and a relatively stable state in colloidal suspensions (Table 1). The absolute value of the ζ-potential in this case was the maximum among all samples, which confirms the greatest colloidal stability (Fig. 3C).

## Discussion

Recently UCNP has become one the best candidates in nanobiomedical research for improved bioimaging and theranostic applications. Incubation of nanoparticles with albumin leads to the formation of PC on their surface. Several approaches have been developed to investigate albumin usage to stabilize nanoparticles and increase their blood circulation time (An & Zhang, 2017). Longer circulation facilitates their accumulation in tumor sites via passive diffusion through the large pores of tumor vasculature or otherwise known as the EPR effect (Barua & Mitragotri, 2014).

In this study, we assembled a new diagnostic nanocomplex based on UCNP coated with $NOBF_4$ and stabilized with a PC layer of BSA. It was essential to determine the optimal ratio between BSA and UCNP-$NOBF_4$ to stabilize the nanoparticles by forming a stable layer of PC. The suspension of BSA with UCNP-$NOBF_4$ promotes a protein concentration dependant formation of PC around the nanoparticles, a factor that was ignored for some time but established recently (Zhang et al., 2017). The results obtained showed the dependence of PC formation on BSA concentration to a certain level of saturation (Fig. 3). This approach takes advantage of the strong electrostatic interactions between positively charged UCNP-$NOBF_4$ and negatively charged BSA (Fig. 3 C).

The present work encourages developing methods to exploit PC or reduce its impact to improve drug-carrying nanosystems' therapeutic effect. It was proven that it is possible to stabilize nanoparticles with a certain protein (albumin), which can prevent further adsorption of plasma proteins and increase nanoparticles' circulation time in the bloodstream, and consequently increase the efficiency of their passive delivery to tumor tissue via the EPR effect (An & Zhang, 2017). Moreover, these nanocomplexes have a high PL intensity in the NIR region within the transparency window of living tissues. Therefore, they are now the subject of further intensive investigation for their potential diagnostic agents.

## Acknowledgments

This research was supported by the Ministry of Education and Science of the Russian Federation (Agreement No. RFMEFI58418X0033).

**References**

AIRES A., OCAMPO S.M., CABRERA D., CUEVA L. DE LA, SALAS G., TERAN F. J., & CORTAJARENA A. L. (2015): BSA-coated magnetic nanoparticles for improved therapeutic properties. Journal of Materials Chemistry B, 3(30), 6239–6247.

AN F.-F. & ZHANG X.-H. (2017): Strategies for Preparing Albumin-based Nanoparticles for Multifunctional Bioimaging and Drug Delivery. Theranostics, 7(15), 3667–3689.

BARUA S. & MITRAGOTRI S. (2014): Challenges associated with penetration of nanoparticles across cell and tissue barriers: A review of current status and future prospects. Nano Today. Elsevier B.V, 9(2), 223–243.

BERN M., SAND K.M.K., NILSEN J., SANDLIE I. & ANDERSEN J.T. (2015): The role of albumin receptors in regulation of albumin homeostasis: Implications for drug delivery. Journal of Controlled Release. Elsevier, 211, 144–162.

BHATTACHARJEE S. (2016): DLS and zeta potential - What they are and what they are not? Journal of Controlled Release, 235, 337–351.

CEDERVALL T., LYNCH I., LINDMAN S., BERGGARD T., THULIN E., NILSSON H., DAWSON K.A. & LINSE S. (2007): Understanding the nanoparticle-protein corona using methods to quantify exchange rates and affinities of proteins for nanoparticles. Proceedings of the National Academy of Sciences of the United States of America, 104(7), 2050–2055.

CHATTERJEE D.K., RUFAIHAH A.J. & ZHANG Y. (2008): Upconversion fluorescence imaging of cells and small animals using lanthanide doped nanocrystals. Biomaterials, 29(7), 937–943.

CHEN D., ZHANG F., LV L., HAN Z., WANG Y., GU Y. & CHEN H. (2017): Bovine Serum Albumin Coated Upconversion Nanoparticles for Near Infrared Fluorescence Imaging in Mouse Model. Journal of Nanoscience and Nanotechnology, 17(2), 932–938.

DEYEV S.M. & LEBEDENKO E.N. (2017): Targeted Bifunctional Proteins and Hybrid Nanoconstructs for Cancer Diagnostics and Therapies. Molecular Biology, 51(6), 788–803.

DOMINGUEZ-MEDINA S., KISLEY L., TAUZIN L.J., HOGGARD A., SHUANG B., D. S. INDRASEKARA A.S., CHEN S., WANG L.Y., DERRY P.J., LIOPO A., ZUBAREV E.R., LANDES C.F. & LINK S. (2016): Adsorption and Unfolding of a Single Protein Triggers Nanoparticle Aggregation. ACS Nano, 10(2), 2103–2112.

DONG A., YE X., CHEN J., KANG Y., GORDON T., KIKKAWA J. M. & MURRAY C.B. (2011): A Generalized Ligand-Exchange Strategy Enabling Sequential Surface Functionalization of Colloidal Nanocrystals. Journal of the American Chemical Society, 133(4), 998–1006.

GENERALOVA A.N., CHICHKOV B.N., KHAYDUKOV E.V. (2017): Multicomponent nanocrystals with anti-Stokes luminescence as contrast agents for modern imaging techniques. Advances in Colloid and Interface Science, 245, 1–19.

GURYEV E.L., SMYSHLYAEVA A.S., SHILYAGINA N.Y., SOKOLOVA E.A., SHANWAR S., KOSTYUK A.B., LYUBESHKIN A.V., SCHULGA A.A., KONOVALOVA E.V., LIN Q., ROY I., BALALAEVA I.V., DEYEV S.M. & ZVYAGIN A.V. (2020): UCNP-based Photoluminescent Nanomedicines for Targeted Imaging and Theranostics of Cancer. Molecules, 25(18), 4302.

HADJIDEMETRIOU M., & KOSTARELOS K. (2017): Nanomedicine: Evolution of the nanoparticle corona. Nature Nanotechnology, 12(4), 288–290.

LI X., ZHANG F., & ZHAO D. (2015): Lab on upconversion nanoparticles: Optical properties and applications engineering via designed nanostructure. Chemical Society Reviews, 44(6), 1346–1278.

LUNDQVIST M. (2013): Tracking protein corona over time. Nature Nanotechnology, 8(10), 701–702.

MAI H.X., ZHANG Y.W., SUN L.D., & YAN C.H. (2007): Highly efficient multicolor up-conversion emissions and their mechanisms of monodisperse NaYF4:Yb,Er core and core/shell-structured nanocrystals. Journal of Physical Chemistry C, 111(37), 13721–13729.

MATSUMURA Y., ODA T. & MAEDA H. (1987): General mechanism of intratumor accumulation of macromolecules: Advantage of macromolecular therapeutics. Japanese Journal of Cancer and Chemotherapy, 14(3 II), 821–829.

NEL A.E., MÄDLER L., VELEGOL D., XIA T., HOEK E.M.V., SOMASUNDARAN P., KLAESSIG F., CASTRANOVA V. & THOMPSON M. (2009): Understanding biophysicochemical interactions at the nano-bio interface. Nature Materials, 8(7), 543–557.

SONG Z., ANISSIMOV Y.G., ZHAO J., NECHAEV A.V., NADORT A., JIN D., PROW T.W., ROBERTS M.S. & ZVYAGIN, A.V. (2012): Background free imaging of upconversion nanoparticle distribution in human skin. Journal of Biomedical Optics, 18(6), 061215.

WANG F., WANG J. & LIU X. (2010): Direct Evidence of a Surface Quenching Effect on Size-Dependent Luminescence of Upconversion Nanoparticles. Angewandte Chemie International Edition, 49(41), 7456–7460.

ZHANG T.X., ZHU G.Y., LU B.Y., ZHANG C.L. & PENG Q. (2017): Concentration-dependent protein adsorption at the nano-bio interfaces of polymeric nanoparticles and serum proteins. Nanomedicine, 12(22), 2757–2769.

ZHENG X., ZHU X., LU Y., ZHAO J., FENG W., JIA G., WANG F., LI F. & JIN D. (2016): High-Contrast Visualization of Upconversion Luminescence in Mice Using Time-Gating Approach. Analytical Chemistry, 88(7), 3449–3454.

ZHOU J., LIU Z., & LI F. (2012): Upconversion nanophosphors for small-animal imaging. Chemical Society Reviews, 41(3), 1323–1349.